

Dispersive Magnetic and Electronic Excitations in Iridate Perovskites Probed with Oxygen K -Edge Resonant Inelastic X-ray Scattering

Xingye Lu,^{1,*} Paul Olalde-Velasco,^{1,†} Yaobo Huang,¹ Valentina Bisogni,^{1,‡} Jonathan Pellicciari,^{1,§} Sara Fatale,² Marcus Dantz,¹ James G. Vale,³ E. C. Hunter,⁴ Johan Chang,⁵ Vladimir N. Strocov,¹ R. S. Perry,^{6,7} Marco Grioni,⁵ D. F. McMorrow,³ Henrik M. Rønnow,⁸ and Thorsten Schmitt^{1,¶}

¹*Research Department Synchrotron Radiation and Nanotechnology,
Paul Scherrer Institut, CH-5232 Villigen PSI, Switzerland*

²*Laboratory for Quantum Magnetism, Institute of Physics,
Ecole Polytechnique Fédérale de Lausanne (EPFL), CH-1015 Lausanne, Switzerland*

³*London Centre for Nanotechnology and Department of Physics and Astronomy,
University College London, Gower Street, London, WC1E 6BT, United Kingdom*

⁴*School of Physics and Astronomy, The University of Edinburgh,
James Clerk Maxwell Building, Mayfield Road, Edinburgh EH9 2TT, United Kingdom*

⁵*Laboratory for Quantum Magnetism, Institute of Condensed Matter Physics (ICMP),
Ecole Polytechnique Fédérale de Lausanne (EPFL), CH-1015 Lausanne, Switzerland*

⁶*ISIS neutron spallation source, Rutherford Appleton Laboratory (RAL),
Harwell Campus, Didcot OX11 0QX, United Kingdom*

⁷*London Centre for Nanotechnology and UCL Centre for Materials Discovery,
University College London, 17-19 Gordon Street, London WC1H 0AH, United Kingdom*

⁸*Laboratory for Quantum Magnetism, Institute of Physics (ICMP),
Ecole Polytechnique Fédérale de Lausanne (EPFL), CH-1015 Lausanne, Switzerland*

(Dated: December 20, 2017)

Resonant inelastic X-ray scattering (RIXS) experiments performed at the oxygen- K edge on the iridate perovskites Sr_2IrO_4 and $\text{Sr}_3\text{Ir}_2\text{O}_7$ reveal a sequence of well-defined dispersive modes over the energy range up to ~ 0.8 eV. The momentum dependence of these modes and their variation with the experimental geometry allows us to assign each of them to specific collective magnetic and/or electronic excitation processes, including single and bi-magnons, and spin-orbit and electron-hole excitons. We thus demonstrated that dispersive magnetic and electronic excitations are observable at the O- K edge in the presence of the strong spin-orbit coupling in the $5d$ shell of iridium and strong hybridization between Ir $5d$ and O $2p$ orbitals, which confirm and expand theoretical expectations. More generally, our results establish the utility of O- K edge RIXS for studying the collective excitations in a range of $5d$ materials that are attracting increasing attention due to their novel magnetic and electronic properties. Especially, the strong RIXS response at O- K edge opens up the opportunity for investigating collective excitations in thin films and heterostructures fabricated from these materials.

Characterizing the elementary excitations in correlated electron systems is an essential prerequisite for obtaining a complete understanding of the underlying electronic interactions and therefore crucial for revealing the origin of emergent phases [1]. Resonant inelastic X-ray scattering (RIXS) has become established in the past decade as a powerful tool for studying the momentum dependence of electronic and magnetic excitations [1]. Of particular interest is RIXS at the transition-metal (TM) $L_{2,3}$ edges. Because of the strong spin-orbit coupling (SOC) in the $2p_{\frac{3}{2},\frac{1}{2}}$ level of the intermediate state, single spin-flip excitations are directly allowed at TM- $L_{2,3}$ edges [2–4], making TM- $L_{2,3}$ RIXS specially suited for investigating the magnetic dynamics in $3d$ (cuprates and iron-pnictides) [2–9, 12–14] and $5d$ (iridates and osmates) systems [8–11, 19].

While the Mott state in cuprates is dominated by strong on-site electron correlation (U), the $J_{\text{eff}} = \frac{1}{2}$ Mott state in $5d^5$ iridates is driven by collaborative strong SOC (~ 0.5 eV) and intermediate U (~ 2 eV) under strong octahedral crystal electric field [18]. Because of their novel

Mott physics and certain parallelism with cuprates, layered iridates (Sr_2IrO_4 and $\text{Sr}_3\text{Ir}_2\text{O}_7$) have attracted substantial research interest [8–11, 18] [Figs. 1(a)–(c)]. More recently, thin films and heterostructures of perovskite iridates have been suggested to host non-trivial topological states [21–23] and triggered a new wave of studies on artificial structures [24–26]. However, measuring elementary excitations using Ir- L RIXS on artificial low-dimensional samples requires longer counting time than that on bulk crystal because 11 keV of X-ray has $\sim 10\mu\text{m}$ [27] of attenuation length while artificial thin film and superlattice are usually much thinner ($\sim 10 - 100\text{nm}$) [7, 8, 25, 26].

RIXS at O- K edge (O $1s$ to O $2p$, ~ 530 eV) offers unique opportunities in probing the elementary excitations in $4d$ and $5d$ TM oxides [12, 13] with high energy resolution (~ 45 meV) [22, 31]. Although O- K RIXS has much smaller attenuation length ($\lesssim 100\text{nm}$) than Ir- L RIXS, a comparison between O- K and Ir- L_3 spectra measured on Sr_2IrO_4 suggests that they have comparable counting efficiency (SFig. 6 in [32]). Therefore, soft x-ray RIXS is a promising method for studying artifi-

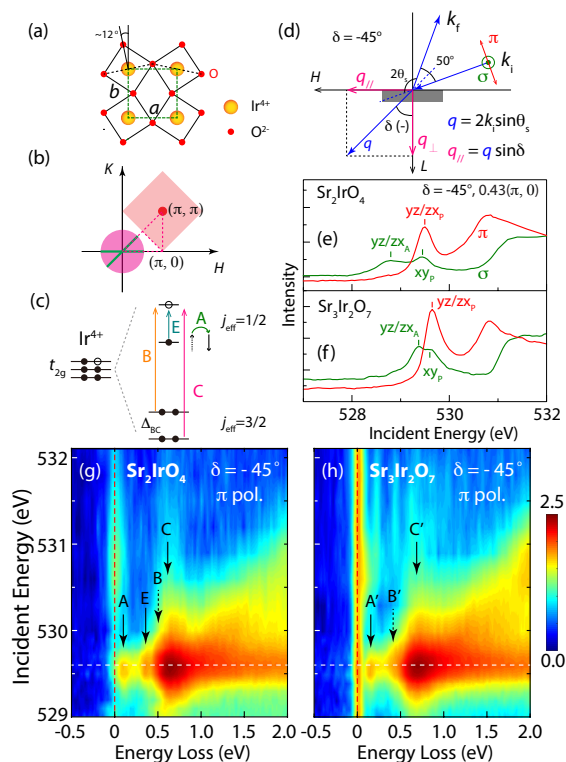


FIG. 1. (color online). (a) Schematic of the distorted IrO plane of Sr₂IrO₄ and Sr₃Ir₂O₇. (b) The corresponding reciprocal space in tetragonal notation. The pink filled circle around Γ point is the momentum coverage of O-*K* RIXS with $2\theta_s = 130^\circ$. The green solid lines mark the two directions $[H, 0]$ and $[H, H]$ we measured. (c) Schematic of elementary excitations of iridates in a single-ion picture. A denotes single magnon, B and C spin-orbit excitons and E electron-hole exciton. Δ_{BC} marks the energy difference between B and C. (d) Schematics of back-scattering RIXS experimental setup. The blue arrows k_i and k_f denote the incident and scattered photons, where the polarizations are shown as red arrow (π) and green circle-dot (σ). The scattering angle is $2\theta_s = 130^\circ$. The projections of q onto two reciprocal axes ($q_{||}$ and q_{\perp}) can be tuned continuously by changing δ . (e)-(f) X-ray absorption spectra at a grazing-incidence angle ($\delta = -45^\circ$) along $[H, 0]$. The probed Ir t_{2g} orbitals (xy , yz and zx) are marked, where the subscripts A and P indicates that orbitals are probed via their hybridization with apical or plane oxygens. (g)-(h) Incident-energy dependence of the elementary excitations of Sr₂IrO₄ and Sr₃Ir₂O₇, measured near the O-*K* edge with π polarization and $\delta = -45^\circ$ along $[H, 0]$.

cial two-dimensional samples [7, 8]. However, given that SOC is absent in O $1s$ level, O-*K* RIXS is expected to be insensitive to single spin-flip excitations [13–15]. This would severely limit the applicability of O-*K* RIXS on iridates and related $5d$ TM oxides, especially thin films and heterostructures fabricated by these materials, where magnetic excitations need to be studied for probing the low energy Hamiltonian [8–11].

Although SOC is absent in O $1s$ orbital, it exists in the Ir $5d$ shell which strongly hybridizes with O $2p$ or-

bitals. This could allow single spin-flip processes at O-*K* edge. Indeed, Kim *et al.* [19] proposed that single spin-flip excitations will be intense at Γ point for O-*K* RIXS if strong SOC is present in TM d orbitals and space inversion symmetry at oxygen sites is broken. However, the symmetry analysis in Ref. [19] is only viable for $q = 0$ and π of a one-dimensional distorted Ir₁-O₁-Ir₂-O₂ periodic arrangement [black dashed line in Fig. 1(a)], which is far from the situations for real iridate materials, such as the Perovskite layered iridates (Sr₂IrO₄ and Sr₃Ir₂O₇) bearing special interests. Later, O-*K* RIXS measurements on a Sr₂IrO₄ thin film reported the possible observation of single magnons at low q but failed to observe the corresponding dispersion that can conclusively determine the single-magnon nature of the observed signal [41]. Therefore, the capability of O-*K* RIXS on probing magnetic excitations of iridates remain to be explored experimentally. In addition, the origin of some collective modes being important for understanding the charge dynamics, is still under debate [9, 42] and requires further experimental studies.

In this study, we use O-*K* RIXS to study layered perovskite iridates Sr₂IrO₄ and Sr₃Ir₂O₇ (the $n = 1$ and 2 of the Ruddlesden-Popper series Sr_{*n*+1}Ir_{*n*}O_{3*n*+1}), which exhibit novel $J_{\text{eff}} = \frac{1}{2}$ Mott physics [9, 16–18]. We unambiguously observe the single magnon dispersion of both samples, thus providing conclusive evidence for the capability of O-*K* RIXS in probing single magnons in $5d$ TM oxides with large SOC. The collective excitonic quasiparticles dispersing between 0.4 – 0.6 eV at the Ir- L_3 edge of Sr₂IrO₄ [9] “dressed” by magnons [19] have also been observed at the O-*K* edge of Sr₂IrO₄ and Sr₃Ir₂O₇. Our results thereby establish the capabilities of O-*K* RIXS in studying dispersive magnetic and electronic excitations in iridates and manifest the strong Ir $5d$ -O $2p$ hybridization in these materials. In addition, dimensionality and temperature dependence of the excitations in Sr₂IrO₄ and Sr₃Ir₂O₇ indicate an electron-hole exciton nature of the sharp dispersive mode [E in Fig. 1(g)].

The Sr₂IrO₄ and Sr₃Ir₂O₇ single crystals used in this study were grown by the flux method [46, 47]. The x-ray absorption (XAS) and RIXS measurements were carried out at the ADDRESS beamline of the Swiss Light Source at the Paul Scherrer Institut [48], with both π and σ polarizations [Fig. 1(d)]. The scattering angle was set to $2\theta_s = 130^\circ$, by which a substantial area of the first Brillouin zone is accessible [pink circle in Fig. 1(b)]. The measurements were performed along two high symmetry directions $[H, 0]$ and $[H, H]$ in tetragonal notation with $a = b \approx 3.9$ Å. The energy resolution for the RIXS measurements was set to 65 meV. The in-plane momentum $q_{||}$ can be tuned continuously by rotating the sample and thereby changing the angle (δ) [Fig. 1(d)].

Figures 1(e) and 1(f) show the XAS spectra for Sr₂IrO₄ and Sr₃Ir₂O₇ measured at a grazing-incidence angle ($\delta = -45^\circ$) [$\mathbf{Q} = 0.43(\pi, 0)$] using π and σ polarizations. The

polarization dependence is determined by the hybridization between Ir $5d t_{2g}$ and O $2p$ orbitals and the matrix elements of the O $1s-2p$ dipole transitions. The σ polarization probes Ir $5d yz/zx$ (xy) orbitals hybridized with $2p_x/2p_y$ orbitals of apical (plane) oxygens. The π polarization predominantly favors the Ir $5d yz/zx$ orbitals via plane-oxygen $2p_z$ orbitals [12, 13, 18]. After having determined the K -edge resonant energies for plane and apical oxygens [yz/zx_A , xy_P and yz/zx_P in Figs. 1(e) and 1(f)], we have performed incident energy dependent RIXS measurements covering these resonant energies. The results measured with π polarization are shown in Figs. 1(g) and 1(h). Clear Raman peaks A/A', E, C/C' observed below 1 eV are identified as single magnons, electron-hole exciton across the charge gap, and spin-orbit excitons, respectively [Fig. 1(c)]. B/B' and BM resolved via multi-gaussian fitting are spin-orbit excitons "dressed" by magnons, and bimagnons, respectively [Fig. 1(c)].

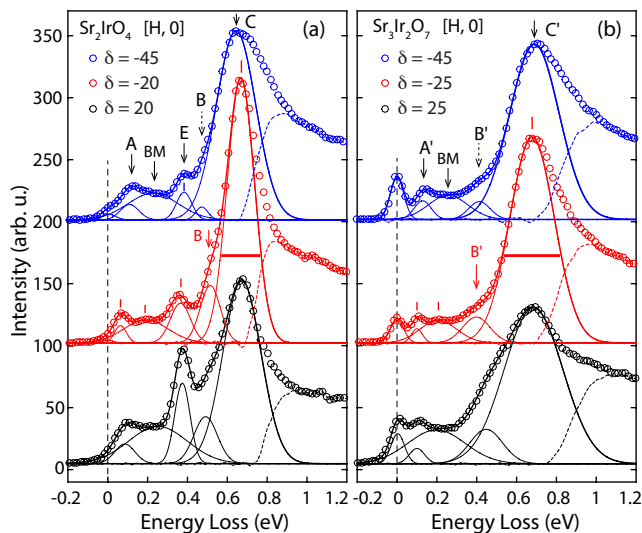


FIG. 2. (color online). Multi-gaussian fitting of the RIXS spectra for (a) Sr_2IrO_4 and (b) $\text{Sr}_3\text{Ir}_2\text{O}_7$. The spectra at three different δ s are shown as colored open circles. From low to high energy loss, the Gaussian peaks (solid curves) denote elastic peak (centered at zero energy loss), single magnon (A/A'), bimagnon (BM), electron-hole exciton (E), excitonic quasiparticle (B/B') and spin-orbit exciton (C/C'). The dashed curves are the residual weight of the fitting.

Figure 2 shows the fitting of selected spectra from grazing incidence [$\delta = -45^\circ$, $0.43(\pi, 0)$] to normal incidence [$\delta = 25^\circ$, $0.25(\pi, 0)$] for Sr_2IrO_4 and $\text{Sr}_3\text{Ir}_2\text{O}_7$ using multiple Gaussians. The systematic fitting resolve all the collective modes below 1 eV and show their incident-angle dependent cross sections. To identify the nature of these collective modes, we have measured the momentum dependence of the RIXS spectra along [H, 0] and [H, H] for both Sr_2IrO_4 and $\text{Sr}_3\text{Ir}_2\text{O}_7$ [Fig. 3], with the incident photon energy tuned to the resonant energy yz/zx_P that enhances all the Raman modes. The spectra shown

in Figs. 2 and 3 are normalized to the charge transfer excitations between 5 and 11 eV [32]. It is remarkable that A and A' show clear dispersions with energy gaps around $\mathbf{Q} = (0, 0)$. The extracted dispersions from the fitting coincide with the magnon dispersions measured by Ir- L_3 RIXS for both Sr_2IrO_4 and $\text{Sr}_3\text{Ir}_2\text{O}_7$ [Fig. 4] [8–11]. Without any doubt, A and A' can be attributed to single magnons, proving that O- K RIXS is sensitive to single magnons in the iridates with strong SOC in $5d$ shell and broken inversion symmetry at oxygen sites [19]. The large magnon gap (~ 90 meV) in $\text{Sr}_3\text{Ir}_2\text{O}_7$ was explained to be driven by strong magnetic anisotropy associated with SOC [10, 11]. The smaller magnon gap in Sr_2IrO_4 (~ 40 meV) is consistent with an Ir- L_3 RIXS report [9] and was described by including an XY anisotropic term [20, 44] into the Heisenberg model described in Ref. [8]. Besides the dispersions, we find that the single magnons persist in the whole momentum space measured with undiminished spectral weight [Figs. 2 and 3], therefore sorting out the momentum dependence of the magnon intensity, which was not settled in previous studies [19, 41].

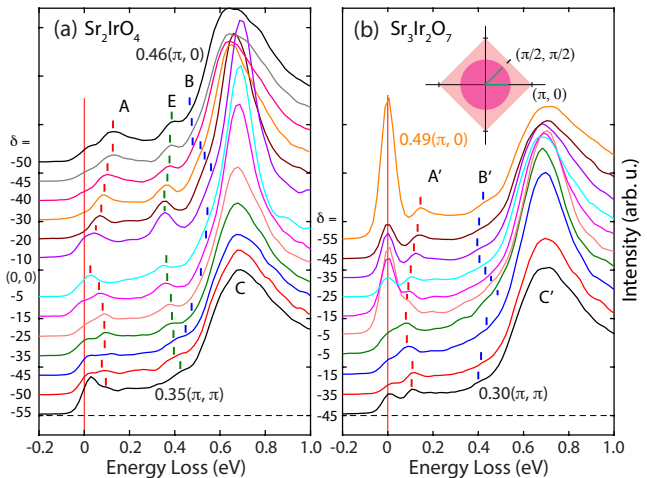


FIG. 3. (color online). Momentum-dependent RIXS spectra along [H, 0] and [H, H] directions for (a) Sr_2IrO_4 and (b) $\text{Sr}_3\text{Ir}_2\text{O}_7$. The inset in (b) illustrates the reciprocal space, where the pink diamond is the magnetic Brillouin zone and the pink filled circle the momentum coverage by O K RIXS. The green lines are the [H, 0] and [H, H] high symmetry directions for RIXS measurements. The red vertical lines mark the zero energy loss positions. The red, green and blue markers indicate the fitted peak energies of the single magnons (A/A'), the electron-hole excitons (E) and the excitonic quasiparticles (B/B'), respectively.

The fitting in Fig. 2 reveals a broad spectral structure at ~ 200 meV for both Sr_2IrO_4 and $\text{Sr}_3\text{Ir}_2\text{O}_7$ [blue squares in Fig. 4], which show similar dispersions to the corresponding single magnons. This feature can be attributed to bimagnons, because (1) their energy scales are consistent with the bimagnons (160 meV for Sr_2IrO_4 and 185 meV for $\text{Sr}_3\text{Ir}_2\text{O}_7$) measured by Raman scatter-

ing [21] and (2) their dispersions are in agreement with those measured by Ir- L_3 RIXS [9–11]. Note that the bimagnons of cuprates measured by O- K RIXS are non-dispersive [14, 15]. The presence of both single magnons and bimagnons indicates that O- K RIXS is a powerful spectroscopic method for studying the magnetic dynamics of iridates.

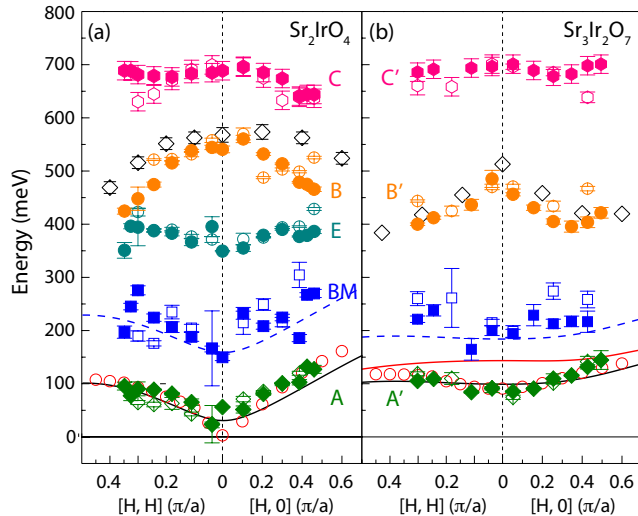


FIG. 4. (color online). Dispersions of the collective modes in (a) Sr_2IrO_4 and (b) $\text{Sr}_3\text{Ir}_2\text{O}_7$ probed by O- K RIXS. From low to high energy loss, the green diamonds, blue squares, cyan circles, orange circles and pink hexagons denote the single magnons (A/A'), bimagnons (BM), electron-hole excitons (E), spin-orbit excitons creating magnons (B/B') and spin-orbit excitons (C/C'), respectively. The solid and open symbols are extracted from the spectra with $\delta < 0$ and $\delta > 0$, respectively [Figs. 1 and 2]. The red open circles are the single magnon energies extracted from previous Ir- L_3 RIXS measurements [8, 11]. The black open diamonds denote the dispersions of the excitonic quasiparticles extracted from Ref. [9, 51]. The black curve in (a) is a theoretical fit of the magnon dispersion using a Heisenberg model reported in [20, 44]. The black and red curves in (b) are transverse and longitudinal magnon dispersions for $\text{Sr}_3\text{Ir}_2\text{O}_7$ using the quantum-dimer model reported in [11]. The blue dashed curves are the expected lower bound of the bimagnon continuum.

In addition to the magnetic excitations, O- K RIXS also reveals the dispersive spin-orbit excitons (B and C) in Sr_2IrO_4 [Fig. 1(c)] as observed in previous Ir- L_3 RIXS experiments [9, 23]. C can be easily attributed to a spin-orbit exciton mode (at ~ 0.7 eV) that exhibits minor dispersion and strong intensity [9, 23]. The mode B finds direct correspondence with the excitonic quasiparticle (spin-orbit exciton “dressed” by magnons) reported in Ref. [9], because of their coincidence in dispersion [Fig. 4(a)] and similarities in band width [Figs. 2(a) and 4(a)]. Furthermore, the intensity of B increases while approaching normal incidence from grazing incidence [Fig. 2(a)]. This incident-geometry dependence of intensity is also consistent with that for the excitonic quasiparticles [9]

and therefore corroborates this identification. The spin-orbit exciton modes B and C arise from the electronic transitions from $j = \frac{3}{2}$ quartet to $j = \frac{1}{2}$ doublet, with B arising mainly from the $|j = 3/2, j_z = \pm 3/2\rangle$ doublet, while C bears mostly $|j = 3/2, j_z = \pm 1/2\rangle$ character. The energy difference between B and C ($\Delta_{BC} \approx 150$ meV) reflects the splitting of the $j = \frac{3}{2}$ band, which is caused by the tetragonal distortion of the IrO_6 octahedra [9].

A similar analysis can be applied to the collective modes B' and C' in $\text{Sr}_3\text{Ir}_2\text{O}_7$. The mode B' is the excitonic quasiparticle in $\text{Sr}_3\text{Ir}_2\text{O}_7$ and C' the spin-orbit exciton mode at higher energy (~ 0.7 eV). B' and C' show similar dispersions to B and C, indicating similar origin and behaviors. However, the energy widths of B' and C' are larger than that for B and C, as evidenced from our fitting analysis in Fig 2. This larger bandwidth is caused by the increase in dimensionality (more adjacent IrO_6 octahedra) in $\text{Sr}_3\text{Ir}_2\text{O}_7$ [37]. The energy of B' is obviously lower than B, meaning that the splitting of the $j = \frac{3}{2}$ states in $\text{Sr}_3\text{Ir}_2\text{O}_7$ is larger ($\Delta_{B'C'} \approx 200$ meV), indicating a larger tetragonal distortion field in $\text{Sr}_3\text{Ir}_2\text{O}_7$ [9, 52].

The sharp collective mode E below 0.4 eV is an intriguing feature whose origin is still under debate [9, 42]. It was firstly suggested to be an electron-hole exciton at the edge of the electron-hole continuum, which has a threshold at about 0.41 eV [9, 52, 53] [Fig. 1(c)]. Alternatively, it was explained as driven by a Jahn-Teller effect with strong SOC [42]. In our measurements, E decreases in intensity with increasing temperature and disappears at 300 K [SFig. 7 of the supplemental material] [32]. This is consistent with the decrease and broadening of the electron-hole continuum threshold at high temperatures as indicated by optical conductivity measurements [53]. The absence of E in $\text{Sr}_3\text{Ir}_2\text{O}_7$ [Figs. 2 and 3] can also be unified in this exciton picture, as the much smaller charge insulating gap (~ 130 meV) and the broader bandwidth of $\text{Sr}_3\text{Ir}_2\text{O}_7$ could smear this exciton and push it to lower energy (~ 100 meV) [37, 54].

The excitonic quasiparticles B and B' ($|j = 3/2, j_z = \pm 3/2\rangle$ to $|j = 1/2, j_z = \pm 1/2\rangle$) deserve special attention. The propagation of the excitonic quasiparticles in the antiferromagnetic context creates flipped spins along their hopping path [9]. Moreover, B and B' are magnetic dd excitations in nature. From the selection rules for dipolar transitions, $\Delta j_z = 0, \pm 1$, it follows that B/B' contains only spin-1 magnetic components, which usually rotates the photon polarization by $\pi/2$, the same as the single spin-flip excitations. This is consistent with previous theoretical calculations [19], which also generate magnetic dd excitations within $5d t_{2g}$ orbitals of Sr_2IrO_4 . Therefore, we conclude that the excitonic quasiparticles observed by O- K RIXS are magnetic orbital excitations “dressed” by magnons. The spin-orbit exciton mode C/C' consists of both non-magnetic and magnetic

components.

The capability of O-*K* RIXS in probing magnetic excitations in iridates is driven by the strong SOC in the Ir 5*d* shell and hybridization between Ir 5*d* t_{2g} and O 2*p* orbitals because spin is not a good quantum number in Ir 5*d* t_{2g} states, indirect electronic transitions between Ir 5*d* t_{2g} orbitals and O 1*s* states via strong O 2*p*-Ir 5*d* hybridization allow flipping of the $j = \frac{1}{2}$ pseudospin and changing of the $j = \frac{3}{2}$ states, in which the former induce single magnons and the latter magnetic (and non-magnetic) *dd* excitations. The role of the space inversion symmetry breaking at oxygen sites need further O-*K* RIXS studies on iridate systems with different Ir-O-Ir bond angles.

In conclusion, our results on Sr₂IrO₄ and Sr₃Ir₂O₇ and their comparison with previous Ir-*L*₃ RIXS results have established the capability of O-*K* RIXS in probing single magnons and excitonic quasiparticles over a substantial part of the first Brillouin zone of layered iridates, which host strong SOC-entangled states in 5*d* orbitals. O-*K* RIXS has high energy resolution for studying most 5*d* TM oxides [31]. Since O-*K* RIXS usually generates strong RIXS response within a small attenuation length, its unique capabilities in probing elementary excitations provide a new method for investigating 5*d* TM oxides, especially for artificial thin films, heterostructures and superlattices.

The work at PSI and EPFL is supported by the Swiss National Science Foundation through its Sinergia network Mott Physics Beyond the Heisenberg Model (MPBH). The work in London is supported by the UK Engineering and Physical Sciences Research Council (Grants No. EP/N027671/1 and No. EP/N034694/1). X. L., V. B. and P. O.-V. acknowledge financial support from the European Community's Seventh Framework Program (FP7/2007-2013) under grant agreement NO. 290605 (COFUND: PSI-FELLOW). J.P. and T.S. acknowledge financial support through the Dysenos AG by Kabelwerke Brugg AG Holding, Fachhochschule Nordwestschweiz, and the Paul Scherrer Institut. J. P. acknowledge financial support by the Swiss National Science Foundation Early Postdoc. Mobility fellowship project number P2FRP2_171824. The work at PSI is partially funded by the Swiss National Science Foundation through the D-A-CH program (SNSF Research Grants No. 200021L 141325). H. M. R. acknowledges financial support from SNSF grant 200020-166298.

* xingye.lu@psi.ch;

Present address: Department of Physics, Beijing Normal University, Beijing 100875, China.

† Present address: Instituto de Física, Benemérita Universidad Autónoma de Puebla, Apdo. Postal J-48, Puebla, Puebla 72570, México.

‡ Present address: National Synchrotron Light Source

II, Brookhaven National Laboratory, Upton, New York 11973, USA.

§ Present address: Department of Physics, Massachusetts Institute of Technology, Cambridge, Massachusetts 02139, USA

¶ thorsten.schmitt@psi.ch

- [1] P. W. Anderson, *Basic Notions of Condensed Matter Physics*, Benjamin-Cummings, London, 1984.
- [2] L. J. P. Ament, M. van Veenendaal, T. P. Devereaux, J. P. Hill, and J. van den Brink, *Rev. Mod. Phys.* **83**, 705 (2011).
- [3] L. J. P. Ament, G. Ghiringhelli, M. Moretti Sala, L. Braicovich, and J. van den Brink, *Phys. Rev. Lett.* **103**, 117003 (2009).
- [4] L. Braicovich, L. J. P. Ament, V. Bisogni, F. Forte, C. Aruta, G. Balestrino, N. B. Brookes, G. M. De Luca, P. G. Medaglia, F. Miletto Granozio, M. Radovic, M. Salluzzo, J. van den Brink, and G. Ghiringhelli, *Phys. Rev. Lett.* **102**, 167401 (2009).
- [5] L. Braicovich, J. van den Brink, V. Bisogni, M. Moretti Sala, L. J. P. Ament, N. B. Brookes, G. M. De Luca, M. Salluzzo, T. Schmitt, V. N. Strocov, and G. Ghiringhelli, *Phys. Rev. Lett.* **104**, 077002 (2010).
- [6] M. Le Tacon, G. Ghiringhelli, J. Chaloupka, M. Moretti Sala, V. Hinkov, M. W. Haverkort, M. Minola, M. Bakr, K. J. Zhou, S. Blanco-Canosa, C. Monney, Y. T. Song, G. L. Sun, C. T. Lin, G. M. De Luca, M. Salluzzo, G. Khaliullin, T. Schmitt, L. Braicovich, and B. Keimer, *Nature Physics* **7**, 725 (2011).
- [7] M. P. M. Dean R. S. Springell, C. Monney, K. J. Zhou, J. Pereira, I. Božović, B. Dalla Piazza, H. M. Rønnow, E. Morenzoni, J. van den Brink, T. Schmitt and J. P. Hill, *Nat. Mater.* **11**, 850 (2012).
- [8] M. P. M. Dean, G. Dellea, R. S. Springell, F. Yakhov-Harris, K. Kummer, N. B. Brookes, X. Liu, Y.-J. Sun, J. Strle, T. Schmitt, L. Braicovich, G. Ghiringhelli, I. Božović and J. P. Hill, *Nat. Mater.* **12**, 1019 (2013).
- [9] W. S. Lee, J. J. Lee, E. A. Nowadnick, S. Gerber, W. Tabis, S. W. Huang, V. N. Strocov, E. M. Motoyama, G. Yu, B. Moritz, H. Y. Huang, R. P. Wang, Y. B. Huang, W. B. Wu, C. T. Chen, D. J. Huang, M. Greven, T. Schmitt, Z. X. Shen and T. P. Devereaux, *Nature Physics* **10**, 883 (2014).
- [10] J. Schlappa, K. Wohlfeld, K. J. Zhou, M. Mourigal, M. W. Haverkort, V. N. Strocov, L. Hozoi, C. Monney, S. Nishimoto, S. Singh, A. Revcolevschi, J.-S. Caux, L. Patthey, H. M. Rønnow, J. van den Brink and T. Schmitt, *Nature* **485**, 82 (2012).
- [11] Ke-Jin Zhou, Yao-Bo Huang, Claude Monney, Xi Dai, Vladimir N. Strocov, Nan-Lin Wang, Zhi-Guo Chen, Chenglin Zhang, Pengcheng Dai, Luc Patthey, Jeroen van den Brink, Hong Ding and Thorsten Schmitt, *Nat. Commun.* **4**, 1470 (2013).
- [12] C. J. Jia, E. A. Nowadnick, K. Wohlfeld, Y. F. Kung, C.-C. Chen, S. Johnston, T. Tohyama, B. Moritz and T. P. Devereaux, *Nat. Commun.* **5**, 3314 (2014).
- [13] M. Guarise, B. Dalla Piazza, H. Berger, E. Giannini, T. Schmitt, H. M. Rønnow, G. A. Sawatzky, J. van den Brink, D. Altenfeld, I. Eremin and M. Grioni, *Nat. Commun.* **5**, 5760 (2014).
- [14] C. Monney, T. Schmitt, C. E. Matt, J. Mesot, V. N. Strocov, O. J. Lipscombe, S. M. Hayden, and J. Chang, *Phys. Rev. B* **93**, 75103 (2016).
- [15] Jungho Kim, D. Casa, M. H. Upton, T. Gog, Young-June

- Kim, J. F. Mitchell, M. van Veenendaal, M. Daghofer, J. van den Brink, G. Khaliullin, and B. J. Kim, *Phys. Rev. Lett.* **108**, 177003 (2012).
- [16] Jungho Kim, M. Daghofer, A. H. Said, T. Gog, J. van den Brink, G. Khaliullin and B. J. Kim, *Nat. Commun.* **5**, 4453 (2014).
- [17] Jungho Kim, A. H. Said, D. Casa, M. H. Upton, T. Gog, M. Daghofer, G. Jackeli, J. van den Brink, G. Khaliullin, and B. J. Kim, *Phys. Rev. Lett.* **109**, 157402 (2012).
- [18] M. Moretti Sala, V. Schnells, S. Boseggia, L. Simonelli, A. Al-Zein, J. G. Vle, L. Paolasini, E. C. Hunter, R. S. Perry, D. Prabhakaran, A. T. Boothroyd, M. Krisch, G. Monaco, H. M. Rønnow, D. F. McMorrow, and F. Mila, *Phys. Rev. B* **92**, 024405 (2015).
- [19] S. Calder, J. G. Vale, N. A. Bogdanov, X. Liu, C. Donnerer, M. H. Upton, D. Casa, A. H. Said, M. D. Lumsden, Z. Zhao, J. -Q. Yan, D. Mandrus, S. Nishimoto, J. van den Brink, J. P. Hill, D. F. McMorrow and A. D. Christianson, *Nat. Commun.* **7**, 11651 (2016).
- [20] B. J. Kim, Hosub Jin, S. J. Moon, J.-Y. Kim, B.-G. Park, C. S. Leem, Jaejun Yu, T. W. Noh, C. Kim, S.-J. Oh, J.-H. Park, V. Durairaj, G. Cao, and E. Rotenberg, *Phys. Rev. Lett.* **101**, 076402 (2008).
- [21] Di Xiao, Wenguang Zhu, Ying Ran, Naoto Nagaosa and Satoshi Okamoto, *Nat. Commun.* **2**, 596 (2011).
- [22] Yige Chen *et al.*, *Nat. Commun.* **6**, 6593 (2015).
- [23] Chen Fang, Ling Lu, Junwei Liu and Liang Fu, *Nat. Phys.* **12**, 936 (2016).
- [24] J. Matsuno, K. Ihara, S. Yamamura, H. Wadati, K. Ishii, V. V. Shankar, Hae-Young Kee, and H. Takagi, *Phys. Rev. Lett.* **114**, 247209 (2015).
- [25] A. Lupascu, J. P. Clancy, H. Gretarsson, Zixin Nie, J. Nichols, J. Terzic, G. Cao, S. S. A. Seo, Z. Islam, M. H. Upton, Jungho Kim, D. Casa, T. Gog, A. H. Said, Vamshi M. Katukuri, H. Stoll, L. Hozoi, J. van den Brink, and Young-June Kim, *Phys. Rev. Lett.* **112**, 147201 (2014).
- [26] J. H. Gruenewald, J. Kim, H. S. Kim, J. M. Johnson, J. Hwang, M. Souri, J. Terzic, S. H. Chang, A. Said, J. W. Brill, G. Cao, H.-Y. Kee, and S. S. A. Seo, *Adv. Mater.* **29**, 1603798 (2017).
- [27] B. L. Henke, E. M. Gullikson, and J. C. Davis, *Atomic Data and Nuclear Data Tables* **54**, 181-342 (1993).
- [28] M. Moretti Sala, M. Rossi, S. Boseggia, J. Akimitsu, N. B. Brookes, M. Isobe, M. Minola, H. Okabe, H. M. Rønnow, L. Simonelli, D. F. McMorrow, and G. Monaco, *Phys. Rev. B* **89**, 121101(R) (2014).
- [29] C. G. Fatuzzo, M. Dantz, S. Fatale, P. Olalde-Velasco, N. E. Shaik, B. Dalla Piazza, S. Toth, J. Pellicciari, R. Fittipaldi, A. Vecchione, N. Kikugawa, J. S. Brooks, H. M. Rønnow, M. Grioni, Ch. Rüegg, T. Schmitt, and J. Chang, *Phys. Rev. B* **91**, 155104 (2015).
- [30] W. S. Lee, S. Johnston, B. Moritz, J. Lee, M. Yi, K. J. Zhou, T. Schmitt, L. Patthey, V. Strocov, K. Kudo, Y. Koike, J. van den Brink, T. P. Devereaux, and Z. X. Shen, *Phys. Rev. Lett.* **110**, 265502 (2013).
- [31] The energy resolution of O-*K* edge RIXS of SAXES spectrometer at ADDRESS beamline is ~ 45 meV with reasonable counting rate. For even higher energy resolving power, see the descriptions of ID32, ESRF, SIX, NSLS II and I21, Diamond.
- [32] See Supplemental Material [url] for details.
- [33] V. Bisogni, L. Simonelli, L. J. P. Ament, F. Forte, M. Moretti Sala, M. Minola, S. Huotari, J. van den Brink, G. Ghiringhelli, N. B. Brookes, and L. Braicovich, *Phys. Rev. B* **85**, 214527 (2012).
- [34] V. Bisogni, M. Moretti Sala, A. Bendounan, N. B. Brookes, G. Ghiringhelli, and L. Braicovich, *Phys. Rev. B* **85**, 214528 (2012).
- [35] G. Jackeli and G. Khaliullin, *Phys. Rev. Lett.* **102**, 017205 (2009).
- [36] Jeffrey G. Rau, Eric Kin-Ho Lee, and Hae-Young Kee, *Annu. Rev. Condens. Matter Phys.* **7**, 195 (2016).
- [37] S. J. Moon, H. Jin, K. W. Kim, W. S. Choi, Y. S. Lee, J. Yu, G. Cao, A. Sumi, H. Funakubo, C. Bernhard, and T. W. Noh, *Phys. Rev. Lett.* **101**, 226402 (2008).
- [38] B. J. Kim, H. Ohsumi, T. Komesu, S. Sakai, T. Morita, H. Takagi, and T. Arima, *Science* **323**, 1329 (2009).
- [39] J. W. Kim, Y. Choi, Jungho Kim, J. F. Mitchell, G. Jackeli, M. Daghofer, J. van den Brink, G. Khaliullin, and B. J. Kim, *Phys. Rev. Lett.* **109**, 037204 (2012).
- [40] Beom Hyun Kim and Jeroen van den Brink, *Phys. Rev. B* **92**, 081105(R) (2015).
- [41] X. Liu, M. P. M. Dean, J. Liu, S. G. Chiužbaian, N. Jaouen, A. Nicolaou, W. G. Yin, C. Rayan Serrao, R. Ramesh, H. Ding and J P Hill, *J. Phys.: Condens. Matter* **27**, 202202 (2015).
- [42] E. M. Plotnikova, M. Daghofer, J. van den Brink, and K. Wohlfeld, *Phys. Rev. Lett.* **116**, 106401 (2016).
- [43] J. G. Vale, S. Boseggia, H. C. Walker, R. Springell, Z. Feng, E. C. Hunter, R. S. Perry, D. Prabhakaran, A. T. Boothroyd, S. P. Collins, H. M. Rønnow, and D. F. McMorrow, *Phys. Rev. B* **92**, 020406(R) (2015).
- [44] D. Pincini, J. G. Vale, C. Donnerer, A. de la Torre, E. C. Hunter, R. Perry, M. Moretti Sala, F. Baumberger, and D. F. McMorrow, arXiv:1703.09051.
- [45] H. Gretarsson, N. H. Sung, M. Höppner, B. J. Kim, B. Keimer, and M. Le Tacon, *Phys. Rev. Lett.* **116**, 136401 (2016).
- [46] G. Cao, J. Bolivar, S. McCall, J. E. Crow, and R. P. Guertin, *Phys. Rev. B* **57**, R11039 (1998).
- [47] G. Cao, Y. Xin, C. S. Alexander, J. E. Crow, P. Schlottmann, M. K. Crawford, R. L. Harlow, and W. Marshall, *Phys. Rev. B* **66**, 214412 (2002).
- [48] G. Ghiringhelli, A. Piazzalunga, C. Dallera, G. Trezzi, L. Braicovich, T. Schmitt, V. N. Strocov, R. Betemps, and L. Patthey, X. Wang and M. Grioni, *Rev. Sci. Instrum.* **77**, 113108 (2006).
- [49] H. Gretarsson, N. H. Sung, J. Porras, J. Bertinshaw, C. Dietl, Jan A. N. Bruin, A. F. Bangura, Y. K. Kim, R. Dinnebier, Jungho Kim, A. Al-Zein, M. Moretti Sala, M. Krisch, M. Le Tacon, B. Keimer, and B. J. Kim, *Phys. Rev. Lett.* **117**, 107001 (2016).
- [50] Xingye Lu, D. E. McNally, M. Moretti Sala, J. Terzic, M. H. Upton, D. Casa, G. Cao, T. Schmitt, *Phys. Rev. Lett.* **118**, 027202 (2017).
- [51] S. Boseggia, PhD Thesis, University College London, 2014, page 184, 193.
- [52] H. Gretarsson, J. P. Clancy, X. Liu, J. P. Hill, Emil Bozin, Yogesh Singh, S. Manni, P. Gegenwart, Jungho Kim, A. H. Said, D. Casa, T. Gog, M. H. Upton, Heung-Sik Kim, J. Yu, Vamshi M. Katukuri, L. Hozoi, Jeroen van den Brink, and Young-June Kim, *Phys. Rev. Lett.* **110**, 076402 (2013).
- [53] S. J. Moon, Hosub Jin, W. S. Choi, J. S. Lee, S. S. A. Seo, J. Yu, G. Cao, T. W. Noh, and Y. S. Lee, *Phys. Rev. B* **80**, 195110 (2009).
- [54] Y. Okada *et al.*, *Nat. Mater.* **12**, 707 (2013).

SUPPLEMENTARY MATERIAL

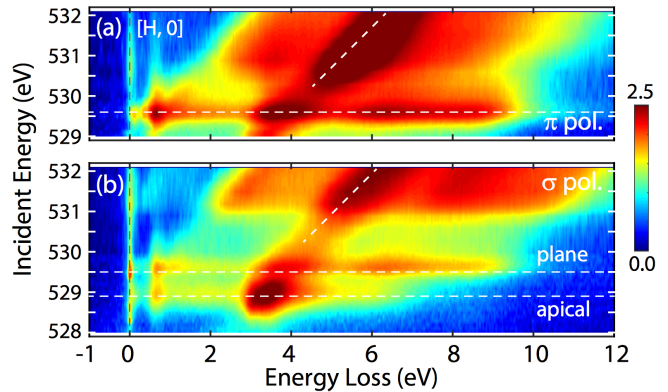
Resonant Inelastic X-ray Scattering at
Transition-Metal L Edge and Oxygen K edge

Resonant inelastic x-ray scattering (RIXS) is a photon-in-photon-out scattering technique suitable for measuring elementary excitations of condensed matter systems [1]. In RIXS, the incident photon energy is tuned to an x-ray absorption edge of certain element to enhance the cross sections for specific elementary excitations [1]. At the transition-metal (TM) $L_{2,3}$ edges, the incident photons excite a $2p$ core electron (with spin σ) into the outer d shell, leaving a core hole in the $2p$ state. Because of the strong spin-orbit coupling (SOC) in TM $2p$ shell, SOC-entangled $2p_{\frac{3}{2}, \frac{1}{2}}$ states are formed, where spin is no longer a good quantum number [2]. In the subsequent relaxation process, an electron with spin $-\sigma$ can therefore fill the core hole. The net result of this RIXS process is a spin-flip excitation. Therefore, single spin-flip excitations are directly allowed at TM- L edge, driven by the strong SOC in the $2p$ core level [2–4]. TM- L RIXS is usually performed at the L_3 edge ($2p_{\frac{3}{2}}$) [5–11].

Different from TM- L_3 edge, oxygen- K (O- K) edge involves O $1s - 2p$ electronic transitions. Since SOC is absent at s level, single spin-flip excitations are assumed to be forbidden at O- K edge [1], as supported experimentally by previous RIXS reports on various $3d$ and $4d$ TM oxides [12–15]. However, considering the strong SOC in $5d$ levels of various $5d$ TM oxides such as iridates and strong hybridization between TM $5d$ orbitals and O $2p$ orbitals [16–18], exploring single spin-flip excitation via O- K RIXS could be possible. A theoretical proposal from Kim *et al.* [19] suggested that single magnons and magnetic orbital excitations could be allowed in Sr_2IrO_4 , because of the strong SOC in Ir $5d$ t_{2g} orbitals and the broken space inversion symmetry at oxygen sites. Despite this, a conclusive experimental study demonstrating the capability of O- K RIXS in probing single spin-flip excitations is still lacking.

Towards this aim, we have performed O- K RIXS measurements on the archetypical iridates Sr_2IrO_4 and $\text{Sr}_3\text{Ir}_2\text{O}_7$ [8, 10, 16–18]. We have shown our key discoveries in the main text. Our results have unambiguously shown that O- K RIXS is sensitive to single magnon and excitonic quasiparticles in the spin-1 channel. In this supplemental material, we show more detailed data to complement our studies on Sr_2IrO_4 and $\text{Sr}_3\text{Ir}_2\text{O}_7$ using O- K RIXS.

Incident Photon Energy Dependent RIXS at
Grazing Incidence



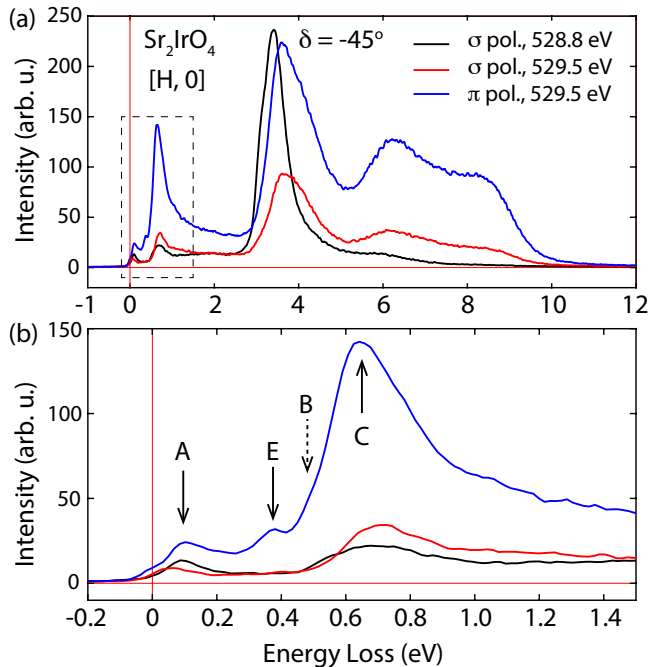
SFigure 1. Incident photon energy dependent elementary excitations of Sr_2IrO_4 , measured near the O- K edge with π and σ polarizations. The measurements were performed with $\delta = -45^\circ$ along tetragonal $[H, 0]$ direction. The diagonal white dashed lines mark the fluorescence lines. The resonant energies corresponding to the absorption peaks are marked by horizontal white dashed lines. The two white dashed lines in (b), ~ 528.8 eV and ~ 529.6 eV, denote the resonant peaks for apical and plane oxygen, respectively.

In Fig. 1 of the letter, we have shown incident photon energy (E_i) dependent RIXS in the low energy loss region ($[-0.5, 2]$ eV) for π polarization at a grazing incident angle ($\delta = -45^\circ$). Here we show in SFigs. 1 to 4 the E_i -dependent RIXS maps and selected spectra measured at resonant energies for both π and σ polarizations in a wide energy loss range ($[-1, 12]$ eV). The E_i ranges cover the O- K absorption peaks [Figs. 1(c) and 1(d) of main text] associated with the Ir t_{2g} yz/zx and xy orbitals [12, 13]. The white dashed lines mark the resonant absorption energies.

SFig. 1 depicts the whole E_i -dependent RIXS map for Sr_2IrO_4 . Besides the Raman features marked in Fig. 1(e), excitations at ~ 3.5 eV, 6.5 eV and 8.8 eV [SFig. 1(a)] containing Raman components have also been observed near the resonant energy associated with the Ir t_{2g} yz/zx orbitals (~ 529.6 eV) using π polarized photons. The excitations at ~ 3.5 eV can be attributed to the main O $2p$ decay channel with strong signature of the dd excitations between Ir t_{2g} and e_g orbitals observed at O- K edge due to the strong O $2p$ -Ir $5d$ hybridization. The excitations above 6 eV can be ascribed to charge transfer excitations. Above the resonant energy, strong fluorescence appears at energy loss above 2 eV.

SFig. 1(b) shows the RIXS energy map measured with σ polarization between $E_i = 528$ and 532 eV. Corresponding to the two resonant absorption peaks in Fig. 1(c), the RIXS map in SFig. 1(b) also shows two resonant energies enhancing different excitations. Both energies enhance the spin-orbit exciton at ~ 0.7 eV but fail to re-

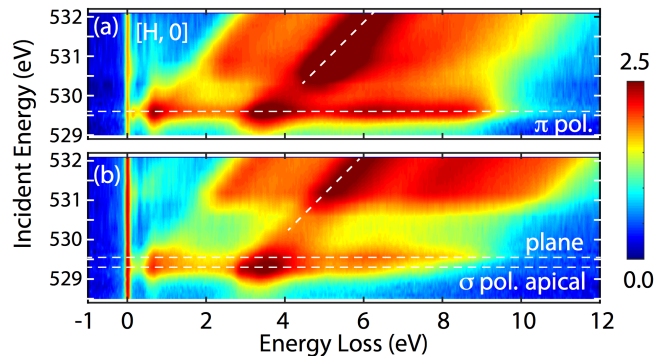
veal the clear Raman features A (~ 0.1 eV) and E (~ 0.4 eV), which have been identified as the single magnon and an exciton across the charge gap as explained in the main text.



SFigure 2. Polarization-dependent RIXS spectra measured at resonant absorption peaks for Sr_2IrO_4 . The corresponding incident energies are marked by horizontal white dashed lines in SFig. 1 and green and red ticks in Fig. 1(c). (a) shows the full energy loss region, while (b) is a zoomed-in view of the rectangular region in (a). Raman features A, E, B, and C are marked by arrows.

To show polarization dependence quantitatively, we compare the RIXS spectra collected at the three resonant energies [white dashed lines in SFig. 1] in SFig. 2. It is clear that all the Raman features are greatly enhanced at the plane-oxygen resonant energy with π polarization [yz/zx_P in Fig. 1(c)], which probes Ir d_{yz}/d_{zx} orbitals through their hybridization with p_z orbitals of plane-oxygen ions [12]. This could be understood considering that all these collective modes propagate within the IrO_2 plane [8, 9]. The charge transfer excitations are also enhanced at yz/zx_P ($E_i \approx 529.6$ eV, π polarization), and they can also be clearly observed when exciting at the plane-oxygen energy with σ polarization that probe the Ir t_{2g} xy orbital [xy_P in Fig. 1(c)]. In contrast, the charge transfer excitations are much weaker in the spectrum measured at the apical-oxygen resonant energy yz/zx_A ($E_i \approx 528.8$ eV, σ polarization). Therefore, we speculate that the charge transfer process occurs mostly within the IrO_2 plane, in agreement with the single-layer structure of Sr_2IrO_4 .

The same data analysis and interpretations can be applied to the polarization dependence of the grazing-



SFigure 3. E_i -dependent elementary excitations for $\text{Sr}_3\text{Ir}_2\text{O}_7$, measured near the O- K edge with π and σ polarizations along $[\text{H}, 0]$ and $[\text{H}, \text{H}]$ directions, with $\delta = -45^\circ$. The diagonal white dashed lines mark the corresponding fluorescence lines. The resonant energies are marked by horizontal white dashed lines. The two white dashed lines at ~ 529.3 eV and ~ 529.5 eV in (b) denote the resonant peaks for apical and plane oxygen, as shown in Fig. 1(d), respectively.

incident spectra for $\text{Sr}_3\text{Ir}_2\text{O}_7$. All the collective excitations favor the plane-oxygen resonant energy with π polarization [yz/zx_P in Fig. 1(d)] [SFIGs. 3 and 4]. Because of the bilayer structure, the difference between the resonant energies yz/zx_P and yz/zx_A decreases to a much smaller value (~ 0.2 eV) than that in Sr_2IrO_4 , as shown in Fig. 1(d) and SFig. 3. The bilayer structure also increases the charge transfer excitations (above 5 eV) probed via the apical-oxygen resonant energy [yz/zx_A in Fig. 1(d)] [SFIG. 4(a)].

Angular (δ) Dependence of the RIXS spectra: Momentum Dispersion

The in-plane momentum can be tuned by changing the sample angles δ and ϕ , where δ controls the magnitude of the projected in-plane momentum (q_{\parallel}) and the azimuthal angle ϕ determines the scattering plane. In our measurements, the momentum directions $[\text{H}, 0]$ and $[\text{H}, \text{H}]$ were reached by fixing ϕ at specific angles. To facilitate our measurements, we tune δ with a step of 5° . The corresponding in-plane momenta along $[\text{H}, 0]$ and $[\text{H}, \text{H}]$ are calculated and shown in Table I, in the unit of (π/a) .

SFigure 5 shows δ dependence of RIXS spectra. SFIGs. 5(a) and 5(b) show RIXS spectra for Sr_2IrO_4 and $\text{Sr}_3\text{Ir}_2\text{O}_7$ at positive and negative sides of δ , which generate consistent dispersions for the collective modes [Fig. 4]. On the other hand, it is well known that RIXS cross section is sensitive to incident geometry. As shown in SFIGs. 5(a) and 5(b), all the collective excitations are clearly observed in negative δ (close to grazing incidence), while they are difficult to be identified and distinguished

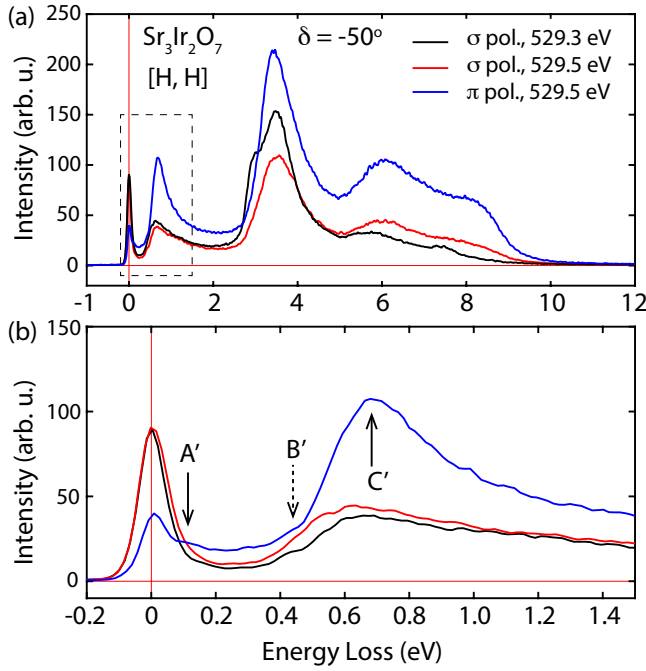


Figure 4. (a) Polarization-dependent RIXS at resonant absorption peaks for $\text{Sr}_3\text{Ir}_2\text{O}_7$. The corresponding incident energies are marked by horizontal white dashed lines in SFig. 3 and green and red ticks in Fig. 1d. (a) is for full energy loss region, while (b) is a zoomed-in view of the rectangular region in (a). The Raman features A', B', and C' are marked by arrows.

from each other in grazing exit side ($\delta > 25^\circ$), where the single magnon (A and A') and the spin-orbit exciton at ~ 0.7 eV (C and C') become broader and less pronounced. However, the excitonic quasiparticles (B and B') are enhanced close to normal incidence ($\delta = 25^\circ$), which is consistent with previous results measured by $\text{Ir-}L_3$ RIXS [9]. All the spectra in Fig. 2, 3 and SFig. 5 are normalized to the charge transfer excitations in the energy range of [5, 11] eV, as indicated by vertical dashed lines in SFig. 5(c).

Comparison between O-K RIXS and Ir- L_3 RIXS

A direct comparison between O-K RIXS and Ir- L_3 RIXS in measuring the same momentum can provide a compelling evidence for the capability of O-K RIXS in probing elementary excitations. For this purpose, we have measured the spectrum for $\mathbf{Q} = (0, 0)$ of Sr_2IrO_4 using both O-K and Ir- L_3 RIXS [SFig. 6]. To make the comparison clear, the spectral intensity in SFig. 6 is plotted in log scale and a constant background (10) is added to the Ir- L_3 spectrum. It is clear that both spectra host similar collective modes at same energies, as marked by pink dashed lines in SFig. 6.

The single magnon exhibits substantial intensity and

TABLE I. Sample angle δ and its corresponding in-plane momentum, which is calculated with the scattering angle $2\theta_s = 130^\circ$, incident energy $E_i = 529.6$ eV and tetragonal lattice parameters $a = b = 3.89\text{\AA}$ [8, 10].

$ \delta $ ($^\circ$)	$q_{//}$ ($1/\text{\AA}$)	$[H, 0](\pi/a)$	$[H, H](\pi/a)$
0	0	0	0
5	0.0423	0.0524	0.0370
10	0.0843	0.1043	0.0738
15	0.1256	0.1555	0.1100
20	0.1659	0.2055	0.1453
25	0.2051	0.2539	0.1795
30	0.2426	0.3004	0.2124
35	0.2783	0.3446	0.2437
40	0.3119	0.3862	0.2731
45	0.3431	0.4248	0.3004
50	0.3717	0.4602	0.3254
55	0.3975	0.4921	0.3480
60	0.4202	0.5203	0.3679

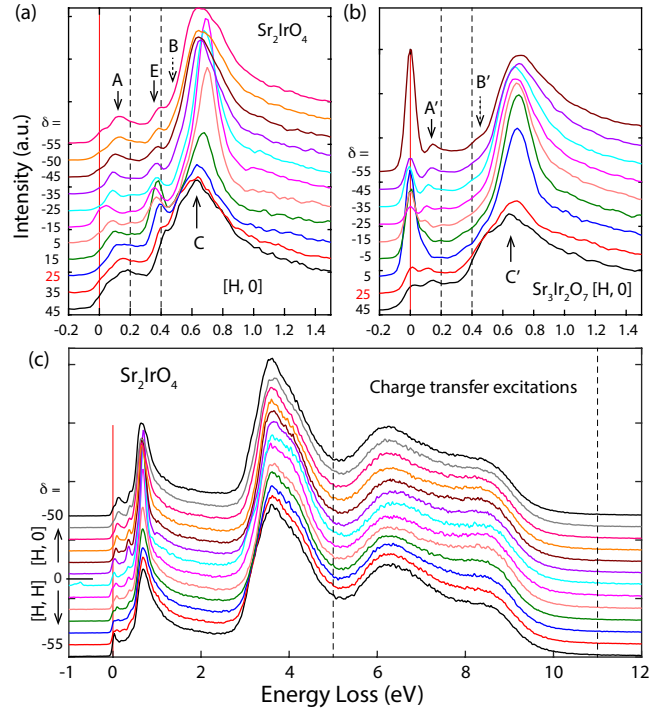
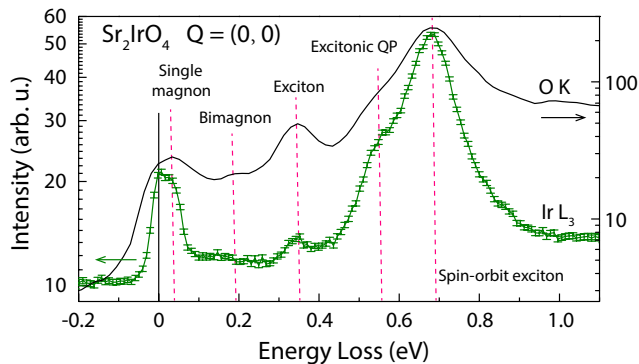


Figure 5. Momentum dependence of the RIXS spectra for Sr_2IrO_4 and $\text{Sr}_3\text{Ir}_2\text{O}_7$. (a) Momentum-dependent RIXS along $[H, 0]$ direction for (a) Sr_2IrO_4 and (b) $\text{Sr}_3\text{Ir}_2\text{O}_7$. The measurements were performed with both positive and negative δ . (c) Full-energy RIXS spectra of Sr_2IrO_4 along $[H, 0]$ and $[H, H]$ directions. All the spectra in (a)-(c) are normalized to the charge transfer excitations between 5 and 11 eV, which is indicated by vertical dashed lines in (c).



SFigure 6. Comparison of the Ir- L_3 and O- K RIXS spectra measured at $Q = (0, 0)$ of Sr_2IrO_4 . The y axis (intensity) is displayed in log scale. The vertical pink dashed lines mark the Raman features revealed at both edges. The spectrum measured by O- K RIXS was collected in 80 minutes of counting time at SAXES, ADDRESS beamline ($\Delta E \approx 65$ meV) with the flux at sample about $6 \times 10^{13}/\text{s}$. The one for Ir- L_3 RIXS was measured in 150 minutes of counting time at 27-ID-B of Advanced Photon Source ($\Delta E \approx 35$ meV), with the flux at sample about $4 \times 10^{13}/\text{s}$, roughly the same as that for O- K RIXS.

forms a peak at ~ 40 meV overlapping with the elastic peak, consistent with recent Ir- L_3 results and the importance of the XY magnetic anisotropy in Sr_2IrO_4 [9, 20]. The feature at about 200 meV could be attributed to bimagnon [21], which is much stronger at O- K edge than that in Ir- L_3 edge [Fig. 3]. We note that the bimagnons are as strong as the single magnons at the O- K edge. This may cause some difficulties in extracting the single magnons, which can be alleviated by better energy resolution, as has recently become available [22]. The spin-orbit exciton at ~ 0.7 eV and the excitonic quasiparticle at ~ 0.55 eV were reported and interpreted in previous reports [8, 9]. The mode at ~ 0.35 eV is an exciton mode at the verge of the electron-hole excitation continuum across the insulating gap [9, 23]. The coincidence of the collective mode energies between O- K and Ir- L_3 RIXS spectra demonstrates that O- K RIXS is capable of measuring single magnons and excitonic quasiparticles.

Temperature Dependence of the Elementary Excitations in Sr_2IrO_4 and $\text{Sr}_3\text{Ir}_2\text{O}_7$

SFigs. 7 and 8 depict the temperature dependence of the elementary excitations below 1 eV for Sr_2IrO_4 and $\text{Sr}_3\text{Ir}_2\text{O}_7$. Upon increasing temperature for Sr_2IrO_4 , the elastic and quasielastic scattering are enhanced. The single magnons decrease in intensity and become less pronounced [SFig. 7]. The excitonic QP at $E \lesssim 0.4$ eV [B in SFig. 2(b)] are heavily damped and disappear at 300 K, while the other excitonic QP at ~ 0.5 eV changes

less and the main spin-orbit exciton at ~ 0.7 eV decrease in intensity by $\sim 20\% - 40\%$ [SFig. 8]. This indicates that the mode is either sensitive to itinerant electrons [23] or based on the in-plane antiferromagnetic structure of Sr_2IrO_4 ($T_N = 245$ K).

$\text{Sr}_3\text{Ir}_2\text{O}_7$ shows similar temperature dependence to Sr_2IrO_4 in single magnons and spin-orbit excitons, except that the sharp excitonic QP mode seen in Sr_2IrO_4 is absent in $\text{Sr}_3\text{Ir}_2\text{O}_7$. Although the single magnons are damped at high temperature, the substantial spectra weight left imply that the damped paramagnons remains at high temperature, which is consistent with previous reports.

* xingye.lu@psi.ch;

Present address: Department of Physics, Beijing Normal University, Beijing 100875, China.

† Present address: Instituto de Física, Benemérita Universidad Autónoma de Puebla, Apdo. Postal J-48, Puebla, Puebla 72570, México.

‡ Present address: National Synchrotron Light Source II, Brookhaven National Laboratory, Upton, New York 11973, USA.

§ Present address: Department of Physics, Massachusetts Institute of Technology, Cambridge, Massachusetts 02139, USA

¶ thorsten.schmitt@psi.ch

- [1] L. J. P. Ament, M. van Veenendaal, T. P. Devereaux, J. P. Hill, and J. van den Brink, *Rev. Mod. Phys.* **83**, 705 (2011).
- [2] L. J. P. Ament, G. Ghiringhelli, M. Moretti Sala, L. Braicovich, and J. van den Brink, *Phys. Rev. Lett.* **103**, 117003 (2009).
- [3] L. Braicovich, L. J. P. Ament, V. Bisogni, F. Forte, C. Aruta, G. Balestrino, N. B. Brookes, G. M. De Luca, P. G. Medaglia, F. Miletto Granozio, M. Radovic, M. Salluzzo, J. van den Brink, and G. Ghiringhelli, *Phys. Rev. Lett.* **102**, 167401 (2009).
- [4] L. Braicovich *et al.*, *Phys. Rev. Lett.* **104**, 077002 (2010).
- [5] M. Le Tacon *et al.*, *Nature Physics* **7**, 725 (2011).
- [6] J. Schlappa, K. Wohlfeld, K. J. Zhou, M. Mourigal, M. W. Haverkort, V. N. Strocov, L. Hozoi, C. Monney, S. Nishimoto, S. Singh, A. Revcolevschi, J.-S. Caux, L. Patthey, H. M. Rønnow, J. van den Brink and T. Schmitt, *Nature* **485**, 82 (2012).
- [7] Ke-Jin Zhou, Yao-Bo Huang, Claude Monney, Xi Dai, Vladimir N. Strocov, Nan-Lin Wang, Zhi-Guo Chen, Chenglin Zhang, Pengcheng Dai, Luc Patthey, Jeroen van den Brink, Hong Ding and Thorsten Schmitt, *Nature Communications* **4**, 1470 (2013).
- [8] Jungho Kim, D. Casa, M. H. Upton, T. Gog, Young-June Kim, J. F. Mitchell, M. van Veenendaal, M. Daghofer, J. van den Brink, G. Khaliullin, and B. J. Kim, *Phys. Rev. Lett.* **108**, 177003 (2012).
- [9] Jungho Kim, M. Daghofer, A. H. Said, T. Gog, J. van den Brink, G. Khaliullin and B. J. Kim, *Nature Communications* **5**, 4453 (2014).
- [10] Jungho Kim, A. H. Said, D. Casa, M. H. Upton, T. Gog, M. Daghofer, G. Jackeli, J. van den Brink, G. Khaliullin,

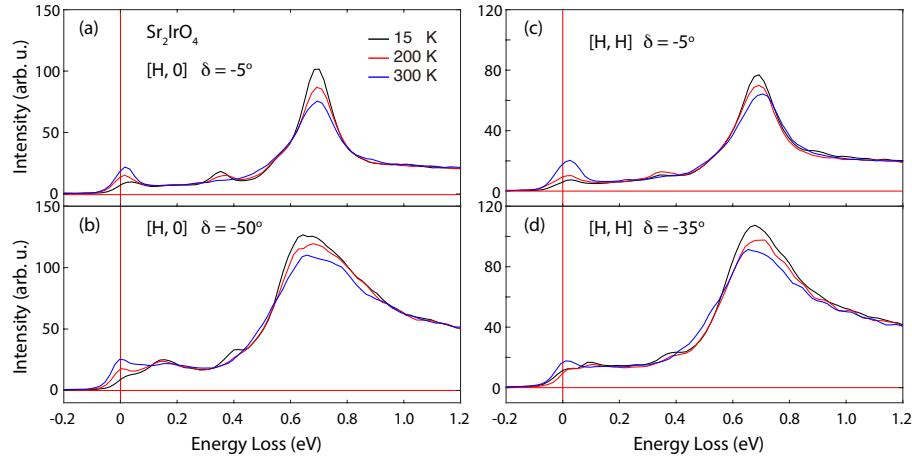


Figure 7. Temperature dependence of magnetic excitations and spin-orbit excitons for Sr_2IrO_4 measured with $\delta = -45^\circ$ along (a) $[\text{H}, 0]$ and (b) $[\text{H}, \text{H}]$ directions. The spectra were collected at $T = 15, 100, 240$ and 300 K.

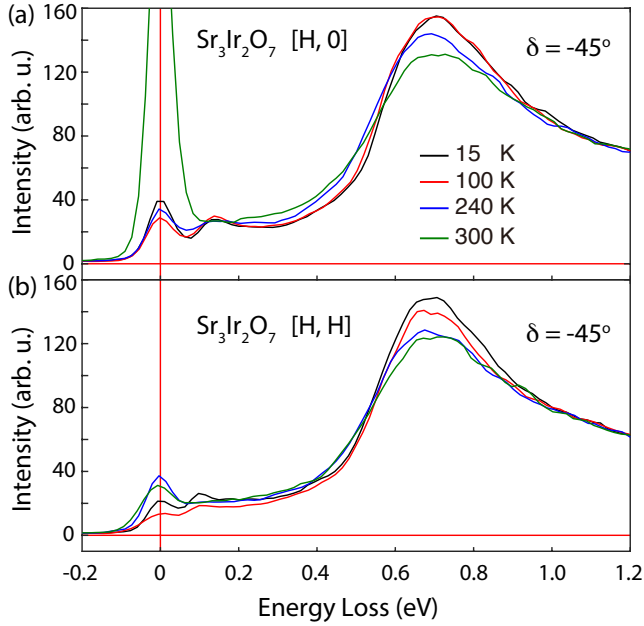


Figure 8. Temperature dependence of magnetic excitations and spin-orbit excitons for $\text{Sr}_3\text{Ir}_2\text{O}_7$ measured with $\delta = -45^\circ$ along (a) $[\text{H}, 0]$ and (b) $[\text{H}, \text{H}]$ directions. The spectra were collected at $T = 15, 100, 240$ and 300 K.

and B. J. Kim, Phys. Rev. Lett. **109**, 157402 (2012).
 [11] M. Moretti Sala, V. Schnells, S. Boseggia, L. Simonelli, A. Al-Zein, J. G. Vle, L. Paolasini, E. C. Hunter, R. S. Perry, D. Prabhakaran, A. T. Boothroyd, M. Krisch, G. Monaco, H. M. Rønnow, D. F. McMorrow, and F. Mila, Phys. Rev. B **92**, 024405 (2015).

[12] M. Moretti Sala, M. Rossi, S. Boseggia, J. Akimitsu, N. B. Brookes, M. Isobe, M. Minola, H. Okabe, H. M. Rønnow, L. Simonelli, D. F. McMorrow, and G. Monaco, Phys. Rev. B **89**, 121101(R) (2014).
 [13] C. G. Fatuzzo, M. Dantz, S. Fatale, P. Olalde-Velasco, N. E. Shaik, B. Dalla Piazza, S. Toth, J. Pellicciari, R. Fittipaldi, A. Vecchione, N. Kikugawa, J. S. Brooks, H. M. Rønnow, M. Grioni, Ch. Rüegg, T. Schmitt, and J. Chang, Phys. Rev. B **91**, 155104 (2015).
 [14] V. Bisogni, L. Simonelli, L. J. P. Ament, F. Forte, M. Moretti Sala, M. Minola, S. Huotari, J. van den Brink, G. Ghiringhelli, N. B. Brookes, and L. Braicovich, Phys. Rev. B **85**, 214527 (2012).
 [15] V. Bisogni, M. Moretti Sala, A. Bendounan, N. B. Brookes, G. Ghiringhelli, and L. Braicovich, Phys. Rev. B **85**, 214528 (2012).
 [16] G. Jackeli and G. Khaliullin, Phys. Rev. Lett. **102**, 017205 (2009).
 [17] Jeffrey G. Rau, Eric Kin-Ho Lee, and Hae-Young Kee, Annu. Rev. Condens. Matter Phys. **7**, 195 (2016).
 [18] B. J. Kim, Hosub Jin, S. J. Moon, J.-Y. Kim, B.-G. Park, C. S. Leem, Jaejun Yu, T. W. Noh, C. Kim, S.-J. Oh, J.-H. Park, V. Durairaj, G. Cao, and E. Rotenberg, Phys. Rev. Lett. **101**, 076402 (2008).
 [19] Beom Hyun Kim and Jeroen van den Brink, Phys. Rev. B **92**, 081105(R) (2015).
 [20] J. G. Vale, S. Boseggia, H. C. Walker, R. Springell, Z. Feng, E. C. Hunter, R. S. Perry, D. Prabhakaran, A. T. Boothroyd, S. P. Collins, H. M. Rønnow, and D. F. McMorrow, Phys. Rev. B **92**, 020406(R) (2015).
 [21] H. Gretarsson, N. H. Sung, M. Höppner, B. J. Kim, B. Keimer, and M. Le Tacon, Phys. Rev. Lett. **116**, 136401 (2016).
 [22] W. S. Lee, S. Johnston, B. Moritz, J. Lee, M. Yi, K. J. Zhou, T. Schmitt, L. Patthey, V. Strocov, K. Kudo, Y. Koike, J. van den Brink, T. P. Devereaux, and Z. X. Shen, Phys. Rev. Lett. **110**, 265502 (2013).
 [23] H. Gretarsson *et al.*, Phys. Rev. Lett. **117**, 107001 (2016).